Spectral Correction for Photovoltaic Module Performance Based on Air Mass and Precipitable Water

Mitchell Lee and Alex Panchula

First Solar, San Francisco, CA, 94105, USA

***Abstract* — A model is proposed for characterizing the effects of spectrum on cadmium telluride and crystalline silicon photovoltaic (PV) modules. It is of simple functional form, allowing it to be easily implemented into standard PV simulation tools. The model corrects for changes in spectrum due to air mass and precipitable water content. The model has module-specific coefficients based on the module's quantum efficiency curve. For modules with similar quantum efficiency curves, the same coefficients can be used. Field performance data of operational PV arrays is used to validate the model. Results illustrate an improvement when compared to existing simple spectral correction methods and suggest that the proposed spectral correction should be included in PV prediction software.**

I. Introduction

Changes in the spectral composition of incoming irradiance due to different atmospheric constituents can have a significant impact on the performance and energy yield of photovoltaic (PV) power plants. Because of varying spectral responsivities, various PV technologies may respond differently under the same spectral conditions. Likewise, the prevailing spectral conditions encountered by a PV array can vary significantly from site to site. Despite the significant impact they can have on PV performance [1]-[6], spectral effects are not accounted for in most software applications commonly used for simulating non-concentrating PV arrays.

Several spectral corrections methodologies have been proposed; however, hurdles have prevented their widespread adoption. King et al. developed the "Sandia Method", an empirically-based spectral correction, determined through outdoor testing, which represents spectral characteristics of PV modules using a fourth order polynomial as function of absolute air mass (AM_a) [7]-[8]. However, later research determined that the correction introduces uncertainty into PV performance predictions. It was speculated that uncertainty in the AM_a based spectral correction was due to atmospheric water vapor [9].

Nelson et al. [1] proposed a parameterization of cadmium telluride (CdTe) PV spectral sensitivity as a function of precipitable water (P_{wat}). The parameterization was derived using the Simple Model of the Atmospheric Radiative Transfer for Sunshine (SMARTS) model with TMY3 data as inputs. SMARTS is an atmospheric model that predicts the spectrum under clear sky conditions [10]. TMY3 files were created by the National Renewable Energy Laboratory (NREL) and provided an hourly annual data set that is representative of typical meteorological conditions and long term irradiance at a particular location [11]. Subsequently, Lee et al. [2] updated the coefficients of the parameterization to model the performance of later generation CdTe modules with improved quantum efficiency (QE) curves. Both papers [1]-[2] presented outdoor PV performance data which corroborates the computationally-derived parameterizations. However, a fundamental limitation of the model is that it cannot be extended to crystalline silicon (c-Si) module types because P_{wat} is not the primary driver of the spectral sensitivity of c-Si PV. In addition, there is a secondary dependence of CdTe spectral sensitivity on AM_a which is absent from the model [3].

We propose a new spectral correction based on AM_a and P_{wat} that is applicable to both CdTe c-Si PV modules. The effectiveness of the proposed spectral model is evaluated using publically available outdoor test data provided by NREL [12]. Results suggest an improvement when compared to existing simple spectral correction methods.

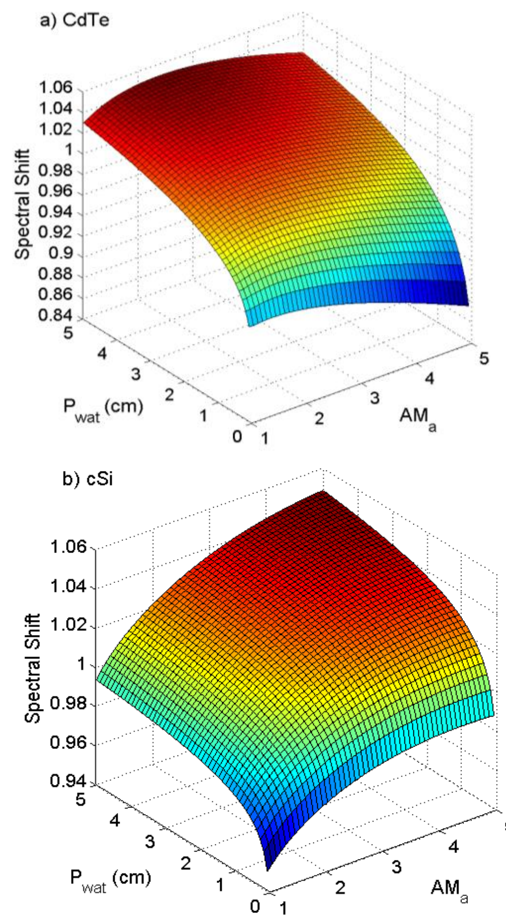

Fig. 1. Sensitivity analysis of M as a function of P_{wat} and AM_a for a) CdTe and b) multi-Si.

II. SPECTRAL MODEL

A. Simulating Spectral Effects Using SMARTS Model

The metric used in this paper to quantify the effects of spectrum on PV performance is called spectral shift (*M*). Spectral shift is often referred to as spectral mismatch in the PV industry. A value of *M* greater than one indicates module power under the prevailing spectrum will be greater than that under broadband irradiance of the same magnitude but distributed according to the ASTM G173 standard. The SMARTS model was used to conduct a multivariate sensitivity analysis on *M* for one multi-crystalline silicon (multi-Si) module and one CdTe module. The modules correspond to Manufacturer 2 Module C and Manufacturer 3 Module D used in the NREL outdoor testing [12].

In accordance with the G173 standard, spectra were simulated on an equatorial facing surface with 37° tilt. All combinations of AM and P_{wat} over the range of 0.1 cm $\leq P_{wat} \leq$ 5 cm and $1 \leq AM \leq 5$ were simulated. The range of wavelengths used in calculations was 280 nm to 2800 nm, which are limits of a typical secondary standard pyranometer. All other parameters input into SMARTS were kept at the G173 standard. Spectral shift was computed for both modules at each AM_a and P_{wat} combination using the generated spectra and module QE curves as inputs. The result of the two variable sensitivity analysis for each module is illustrated in Fig. 1.

B. Parameterization of SMARTS Output

M falls along a continuous 3D surface as a function of AM_a and P_{wat}. The smoothness of the surfaces suggested that they could be easily parameterized. Multiple linear regression was applied using a variety of test functions. Represented in (1) is a functional form that provided a high level of accuracy while remaining relatively simple. The module-specific coefficients are presented in Table I.

$$M = b_0 + b_1 \cdot AM_a + b_2 \cdot p_{wat} + b_3 \cdot \sqrt{AM_a} + b_4 \cdot \sqrt{p_{wat}} + b_5 \cdot \frac{AM_a}{\sqrt{p_{wat}}} \quad (1)$$

For the CdTe module, the coefficient of determination (R^2) between the SMARTS simulation and the regression output was 0.9986 and the mean absolute error (MAE) was 7.7×10^{-4}. The maximum difference between the SMARTS output and the regression was 0.0090. For the multi-Si module, the R^2 between

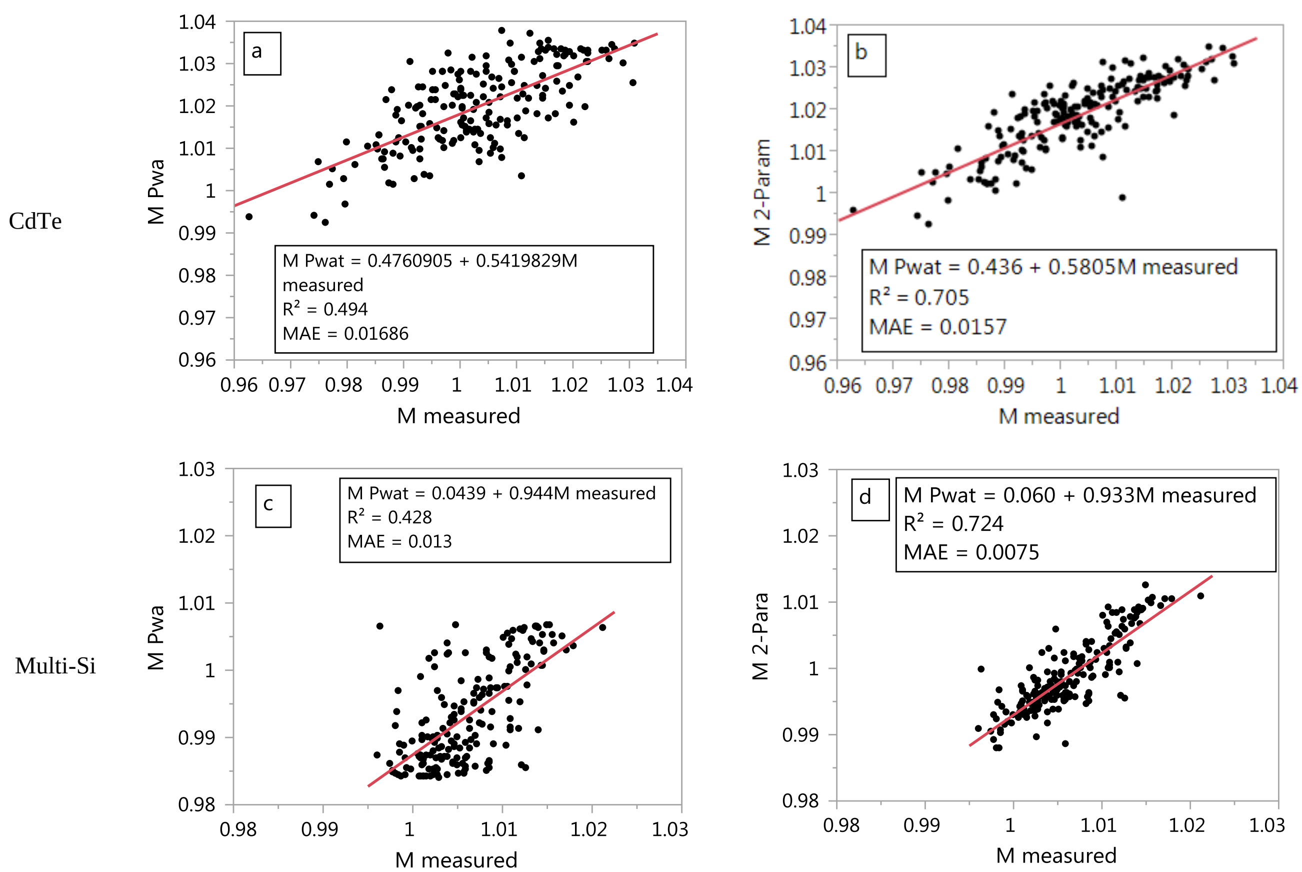

Fig. 2. a) CdTe spectral correlation proposed by [1] versus measured *M* for the CdTe module. b) *M* estimated using (1) versus measured *M* for the CdTe module. c) "Sandia" spectral correction [7]-[8], versus measured *M* the multi-Si module. d) *M* estimated using (1) versus measured *M* for the multi-Si module. All *M* data is of daily resolution and GHI weighted.

the SMARTS simulation and the regression fit was 0.9993 and the MAE was 2.97×10^{-4}. The maximum difference between the SMARTS output and the regression was 0.0047.

TABLE I: PARAMETERIZATION COEFFICIENTS

Module	b_0	b_1	b_2	b_3	b_4	b_5
CdTe	0.7946	-0.05423	-0.01319	0.1724	0.08372	-0.004376
Multi-Si	0.8409	-0.02754	-0.00792	0.1357	0.03802	-0.002122

C. Comparison of Parameterization to Existing Models

The proposed parameterization for the CdTe module was compared to the P_{wat} only model proposed by Nelson et al [1]. In order to do so, (1) was evaluated with the CdTe coefficients for P_{wat} between 0.1 cm and 5 cm (interval of 0.1 cm) and AM_a fixed to the ASTM standard of 1.5. The P_{wat}-only model was evaluated over the same range of P_{wat}. The two models produced roughly equivalent results. The MAE between the two models was 0.0039 and the maximum difference between the two models was 0.0053.

The P_{wat} and AM_a parameterization for the multi-Si module was held at a P_{wat} equal to the G173 standard, 1.42 cm, and was compared to the Sandia AM_a-only correction. The Sandia coefficients for the module were provided by Marion et al. [12]. The models produced similar results, with the mean absolute error between the two models was 0.0039 with the maximum difference between the two models being 0.0062

III. FIELD VALIDATION

Publically available NREL data for test sites in Golden, Colorado; Cocoa, Florida; and Eugene, Oregon, have been analyzed in an attempt to validate the correlation developed using SMARTS [12]. Golden, Köppen Dfb, is warm summer continental or hemiboral climate; Cocoa, Köppen Cfa, is a humid subtropical climate; and Eugene, Köppen Csb, is a cool-summer Mediterranean climate. The data sets contain time series I-V characteristics of the PV modules and corresponding meteorological data at each location. The modules are all fixed tilt, oriented south, with their tilt approximately equal to the latitude of their location. At Eugene and Cocoa, the data was recorded at five minute intervals, whereas at Golden, data was recorded at fifteen minute intervals.

Among other PV technologies, there was one CdTe and three multi-Si modules at each site. This study is limited to the CdTe module, Manufacturer 3 Model D, and multi-Si module, Manufacturer 2 Model C. The particular multi-Si module was chosen for analysis because it was cleaned at regular intervals.

The ratio of module short circuit current (I_{sc}) to plane of array irradiance (POA) as measured using a Kipp & Zonen CMP 22 is used to estimate the effects of spectrum. The ratio has been normalized by dividing by I_{sc} at 1000 W/m^2 as tested according to the Sandia Array Performance Model under outdoor conditions [7]. The module I_{sc} was corrected for the effects of temperature using a linear temperature coefficient. The module I_{sc} was also corrected for angle of incidence (AOI) effects using the Sandia Model [7]-[8]. For incidence angles less than 29°, AOI losses were set to zero to reduce uncertainty which results from the Sandia Model's use of a polynomial fit. The I_{sc} temperature coefficients and AOI response coefficients were measured after field deployment and were made available by [12]. For the CdTe modules, I_{sc} was corrected for soiling losses using the estimates provided by the data set. A soiling correction was not necessary for the multi-Si modules because they were cleaned regularly. In an effort to reduce noise, analysis was limited to when irradiance was greater than 200 W/m^2, AOI effects were less than one percent, and clearness index (K_t) was between 0.7 and 1.0.

The meteorological data at the site was used to estimate spectral shift for both the multi-Si and CdTe modules. For the CdTe modules, spectral shift was estimated using (1) with the appropriate coefficients from Table I, and also by using the P_{wat}-only parameterization proposed by [1]. For the multi-Si modules, spectral effects were estimated using (1) and by using the AM_a-only correction proposed by [7]-[8]. P_{wat} was estimated using relative humidity (*RH*) and ambient temperature (T_{amb}) measurements according to the correlation

TABLE II: LINEAR REGRESSION OF OUTDOOR TESTING DATA

Site, Module	One Parameter Spectral Correlation	Two Parameter Spectral Correlation
Cocoa, FL: CdTe	$M_{P_{wat}} = 0.5420 \cdot M_{measured} + 0.476$ $MAE = 0.0169; R^2 = 0.494$	$M_{2-Param} = 0.5805 \cdot M_{measured} + 0.436$ $MAE = 0.0157; R^2 = 0.705$
Cocoa, FL: multi-Si	$M_{AM_a} = 0.9435 \cdot M_{Measured} + 0.0439$ $MAE = 0.0130; R^2 = 0.428$	$M_{2-Param} = 0.9326 \cdot M_{measure} + 0.0603$ $MAE = 0.00749; R^2 = 0.724$
Eugene, OR: CdTe	$M_{p_{wat}} = 0.536 \cdot M_{measured} + 0.476$ $MAE = 0.0188; R^2 = 0.445$	$M_{2-Param} = 0.638 \cdot M_{measured} + 0.373$ $MAE = 0.0162; R^2 = 0.598$
Eugene, OR: multi-Si	$M_{AM_a} = 1.00292 \cdot M_{measured} - 0.0038$ $MAE = 0.00406; R^2 = 0.696$	$M_{2-Param} = 0.767 \cdot M_{measured} + 0.2303$ $MAE = 0.00306; R^2 = 0.817$
Golden, CO: CdTe	$M_{P_{wat}} = 0.7051 \cdot M_{measured} - 0.28836$ $MAE = 0.00827; R^2 = 0.712$	$M_{2-Param} = 0.7266 \cdot M_{measured} + 0.258$ $MAE = 0.0150; R^2 = 0.706$
Golden, CO: multi-Si	$M_{AM_a} = 0.0360 \cdot M_{measured} + 0.956$ $MAE = 0.00955; R^2 = 0.001$	$M_{2-Param} = 0.561 \cdot M_{measured} + 0.424$ $MAE = 0.01256; R^2 = 0.356$

proposed by [14]-[15]. Air mass was estimated from zenith angle using the method proposed by [16].

The sub-hourly time series data of measured and predicted spectral shift was aggregated to daily resolution using global horizontal irradiance (GHI) weighted averages. For both the CdTe and the multi-Si modules at each site, predicted daily spectral shift, as calculated using the existing and newly proposed spectral correction methodologies, was plotted against measured spectral shift. The results at Cocoa are included as Fig. 2. The results of the linear regression for all three locations are included in Table II.

Both Fig. 2 and Table II illustrate that the two parameter spectral correction as good as, or better than, the existing one parameter models in capturing the effects of spectral shift on

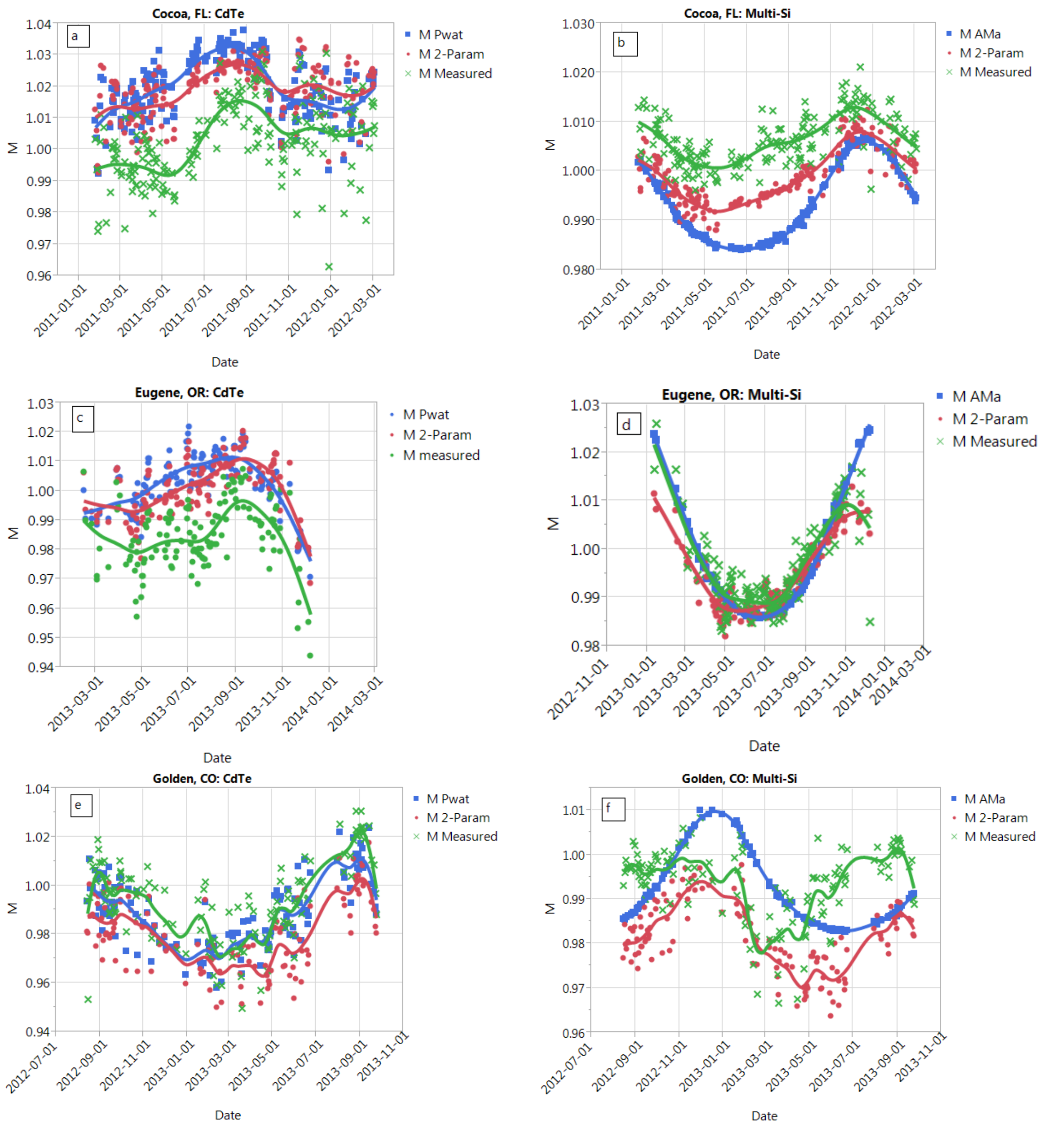

Fig. 3. Time series of measured and modeled M for: a) CdTe module at Cocoa, FL; b) multi-Si module at Cocoa, FL; c) CdTe module at Eugene, OR; d) multi-Si module at Eugene, OR; e) CdTe module at Golden, CO; and f) multi-Si module at Golden, CO. For the CdTe modules, M was estimated using the (1) and the P_{wat}-only spectral corrections. For the c-Si modules, M was estimated using the (1) and the AM_a-only spectral corrections.

module performance. The two parameter spectral correction resulted in the most improvement in Cocoa, Florida. For the CdTe module, the R^2 of the linear fit between M predicted and M measured improved from 0.494 to 0.705. For the multi-Si module, the R^2 improved from 0.428 to 0.724, and the MAE was significantly reduced from 0.13 to 0.0075. At Eugene, the two parameter correlation resulted in a significant improvement in the R^2 between the modeled and measured spectral effects. At Golden, for CdTe the R^2 between the modeled and measured spectral effects was roughly equivalent for the two parameter model and the P_{wat}-only spectral correction. For both models the statistical relationship is strong, with R^2 being greater than 0.70 in both cases. For the multi-Si module in Golden, there was no statistical relationship between the measured M and M estimated using AM_a-only spectral correction. However, using the P_{wat} and AM_a spectral correction increased the R^2 from 0.001 to 0.356, signifying a statically significant, but weak relationship.

Illustrated in Fig. 3 are time series plots of measured M along with the two parameter spectral correction determined from (1) and the appropriate one parameter spectral correction. In Fig. 3, the left column of subplots are for the CdTe modules, and the right are for the multi-Si modules. Each row is for a different test location: subplots (a-b) are for Cocoa subplots (c-d) are for Eugene, and subplots (e-f) are for Golden. Fig. 3(a, c, e) illustrates that for the CdTe module at each site there is good agreement among measured spectral shift, spectral shift modeled using P_{wat} only, and spectral shift modeled using P_{wat} and AM_a.

Fig. 3(b, d) shows that for multi-Si module in Cocoa and Eugene there is also good agreement between the measured spectral shift and spectral shift modeled using P_{wat} and AM_a. However, in both Cocoa and Eugene spectral shift modeled using AM_a only had the correct seasonal trend, but overestimated seasonal variation and failed to capture shorter term variation in spectral shift.

As illustrated by Fig. 3f, for the multi-Si module at Golden there was no relationship between measured spectral shift and spectral shift as estimated using the AM_a-only correlation. Yet, it appears that the two parameter spectral correction is capturing some of the shorter term variation in performance. However, it is not accurately capturing seasonal variation, suggesting that the effects of AM_a are being over weighted. Thus, Fig. 3f provides context for the statically significant, but weak relationship seen in Table II.

Fig. 3(a, c) shows that there is an offset between measured and predicted performance of the CdTe modules in Cocoa and Eugene. While the two parameter and P_{wat}-only spectral corrections are in strong agreement, there is an offset of one to two percent between the modeled and the measured spectral shift. This explains the high overall MAE seen in Table II for the CdTe modules in Cocoa and Eugene. As shown in Fig. 3(b), for the multi-Si PV module in Eugene, there was a similar, but smaller, offset between the two parameter model and measured spectral shift.

Nonetheless, it is difficult to differentiate between model bias and measurement inaccuracy. As previously stated, the nameplate I_{sc} of the PV modules was used to normalize the measured spectral shift. However, the nameplate I_{sc} values were tested through outdoor field testing that does not account for the difference between the prevailing P_{wat} and the G173 standard. As a result, the I_{sc} of the PV modules could have been over or under estimated, causing the offset between measured and modeled spectral shift.

CONCLUSION

This paper presented a newly developed model for characterizing the effects of spectrum on PV modules. The model corrects for changes in spectrum due to air mass and precipitable water content. The model has module-specific coefficients based on the module's quantum efficiency curve. For modules with similar quantum efficiency curves, the same coefficients can be used. Module specific coefficients are calculated through the use of a sensitivity analysis in SMARTS. This paper focuses on CdTe and multi-Si PV modules; however, given the similarity in the quantum efficiency curves between mono-Si and multi-Si PV modules, the proposed spectral model can also be applied to mono-Si. This is done through the generation of module-specific coefficients following the procedure outlined in Section II.

Analysis of publically available data from outdoor PV tests arrays demonstrated that the computationally derived model captured variation in PV module performance due to spectrum. Results illustrate an improvement when compared to existing simple spectral correction methods based on P_{wat}–only or AM_a-only, and suggest that the proposed spectral correction should be included in PV prediction software. We recommend that PV prediction software include this spectral correction. A preliminary version of the proposed spectral correction, with default coefficients for CdTe, multi-Si, and mono-Si PV modules, is available in PVLIB 1.31. PVLIB is publically available set of documented functions for simulating the performance of photovoltaic energy systems in both the MATLAB and Python programing languages [17]. The finalized spectral correction will be available in a future version of PVLIB.

REFERENCES

[1] L. Nelson, M. Frichtl, and A. Panchula, "Changes in cadmium telluride photovoltaic performance due to spectrum," *IEEE Journal of Photovoltaics*, vol. 3, No. 1, pp. 488-493, 2013.

[2] M. Lee, L. Ngan, W. Hayes, and A.F. Panchula, "Understanding Next Generation Cadmium Telluride Photovoltaic Performance due to Spectrum", New Orleans, 2015.

[3] M. Lee, L. Ngan, W. Hayes, and A.F. Panchula, "Comparison of the Effects of Spectrum on Cadmium Telluride and Monocrystalline Silicon Photovoltaic Module Performance", New Orleans, 2015.

[4] M. Schweiger and W. Herrmann, "Comparison of Energy Yield Data of Fifteen PV Module Technologies Operating in Four Different Climates" in *42nd IEEE Photovoltaic Specialists Conference*, New Orleans, 2015.

[5] G.S. Kinsey, "Spectrum sensitivity, energy yield, and revenue prediction of PV modules," *IEEE Journal of Photovoltaics*, vol. 5, no.1, pp. 258-262

[6] B.C Duck and C.J. Fell, "Comparison of Methods for Estimating the Impact of Spectrum on PV Output," in *42nd IEEE Photovoltaic Specialists Conference*, New Orleans, 2015.

[7] D. King, W. Boyson, and J. Kratochvill, *Photovoltaic Array Performance Model, SAND2004-3535*. Albuquerque, New Mexico: Sandia National Laboratories, 2004.

[8] D. King, J. Kratochvill, and W. Boyson, "Measuring solar spectral and angle-of-incidence effects on photovoltaic modules and solar irradiance sensors," in *26th IEEE Photovoltaic Specialists Conference*, 1997, p. 1113 – 1116.

[9] K.A. Klise, C.W. Hansen, and J.S. Stein, "Dependence on geographic location of air mass modifiers for photovoltaic module performance models," in *42nd IEEE Photovoltaic Specialists Conference*, New Orleans, 2015.

[10] C. Gueymard, "SMARTS, a simple model of the atmospheric radiative transfer of sunshine: Algorithms and performance assessment" Florida Sol. Energy Center, Cocoa, FL, Tech. Rep. FSEC-PF-270-95, 1995.

[11] S. Wilcox, W. Marion, "Users Manual for TMY3 Data Sets", National Renewable Energy Laboratory NREL/TP-581-43156, 2008.

[12] W. Marion, A. Anderberg, C. Deline, S. Glick, M. Muller, G. Perrin, *et al*., "User's Manual for Data for Validating Models for PV Module Performance," National Renewable Energy Laboratory NREL/TP-5200-61610, 2014.

[13] B. Marion, "Influence of atmospheric variations on photovoltaic performance and modeling their effects for days with clear skies," in *38th IEEE Photovoltaic Specialists Conference*, 2012, p. 3402–3407.

[14] C. Gueymard, "Analysis of Monthly Average Atmospheric Precipitable Water and Turbidity in Canada and Northern United States," Solar Energy, vol. 53, No.1, pp. 57-71, 1994.

[15] C. Gueymard, "Assessment of the Accuracy and Computing speed of Simplified Saturation Vapor Equations Using a New Reference Dataset," Journal of Applied Meteorology, vol. 32, pp 1294-1300, 1993.

[16] F. Kasten, and A. Young, "Revised optical air mass tables and approximation formula," Applied Optics vol. 28, issue 22, pp. 4735-4738, 1989.

[17] Sandia National Laboratories, PV Performance Modeling Collaborative, PV_LIB Toolbox, (2015). [Online]. Available: https://pvpmc.sandia.gov/applications/pv_lib-toolbox/